Hair cycle-dependent expression of corticotropin-releasing factor (CRF) and CRF receptors in murine skin

B. ROLOFF,*,† K. FECHNER,* A. SLOMINSKI,‡,[1] J. FURKERT,* V. A. BOTCHKAREV,† S. BULFONE-PAUS,§ J. ZIPPER,* E. KRAUSE,* AND R. PAUS†

*Institute of Molecular Pharmacology, Berlin, Germany; †Department of Dermatology, Charité, Humboldt University, Berlin, Germany; ‡Department of Pathology, Loyola University Medical Center, Maywood, Illinois 60153, USA; and §Institute of Immunology, Free University of Berlin, Berlin, Germany

ABSTRACT **We demonstrate the presence and hair cycle-dependent expression of corticotropin-releasing factor (CRF) and CRF receptors (CRF-R) in C57BL/6 mouse skin. To correlate this with a physiological, developmentally controlled tissue remodeling process, we have analyzed CRF and CRF-R expression during defined stages of the murine hair cycle with its rhythmic changes between growth (anagen), regression (catagen), and resting (telogen). Using reversed-phase HPLC combined with two independent anti-CRF radioimmunoassays, we have identified CRF in murine skin. Maximal CRF levels were found in anagen III-IV skin, and minimal values were detected in catagen and telogen skin. By immunofluorescence, maximal CRF immunoreactivity (CRF-IR) was seen in the basal epidermis, nerve bundles of skin, the outer root sheath and matrix region of anagen IV-VI follicles, and in defined sections of their perifollicular neural network, whereas catagen and telogen skin displayed minimal CRF-IR. Using quantitative autoradiography and ^{125}I-CRF as a tracer, high-affinity binding sites for CRF were detected in murine skin. The highest density of specific binding sites was detected in the panniculus carnosus, the epidermis, and the hair follicle. CRF-R type 1 (CRF-R1) IR was detected by immunohistology mainly in the outer root sheath, hair matrix, and dermal papilla of anagen VI follicles, as well as in the inner and outer root sheaths of early catagen follicles. CRF-R1 expression was also hair cycle dependent. Therefore, in normal murine skin, the CRF-CRF-R signaling system may operate as an additional neuroendocrine pathway regulating skin functions, possibly in the context of cutaneous stress responses.—Roloff, B., Fechner, K., Slominski, A., Furkert, J, Botchkarev, V. A., Bulfone-Paus, S., Zipper, J., Krause, E., Paus, R. Hair cycle-dependent expression of corticotropin-releasing factor (CRF) and CRF receptors in murine skin. *FASEB J.* 12, 287–297 (1998)**

Key Words: stress · hair growth · C57BL/6 mouse

CORTICOTROPIN-RELEASING FACTOR (CRF),[2] CRF receptors (CRF-R), and proopiomelanocortin (POMC) are components of the main adaptive response to systemic stress (1–4). CRF, a main regulator of pituitary POMC peptide production, is a 41-amino acid peptide synthetized by cleavage from a large 191-amino acid precursor (2). The CRF gene has two exons, separated by an intron whose prohormone sequence is located in exon 2 (5). CRF exerts its bioregulatory function via activation of CRF-R. Two distinct gene subfamilies encoding CRF-R were cloned, which share high sequence homology and belong to the seven-transmembrane receptor protein family, coupled to the Gs signaling protein (6–9). In addition to the brain and pituitary (6, 9), the CRF-R1 (CRF-R type 1) gene is also transcribed in skin (10, 11), although its cutaneous site of expression is unknown. CRF-R2 includes the CRF-R2α, found predominantly in the brain, and CRF-R2β, which is expressed in heart and skeletal muscle (7, 8).

It has recently been proposed that mammalian skin may contain an equivalent of the 'hypothalamic-pituitary axis' that regulates skin responses to stress (4). This hypothesis is supported by the fact that the skin, which is a recognized target for melanocyte-stimulating hormone (MSH) and adrenocorticotropin (ACTH) bioregulation, expresses the POMC gene and produces POMC peptides like MSH, ACTH, and

[1] Correspondence: Department of Pathology, Loyola University Medical Center, 2160 S. First Ave., Maywood, IL 60153, USA. E-mail: aslom@wpo.it.luc.edu

[2] Abbreviations: ACTH, adrenocorticotropin; BSA, bovine serum albumin; CRF, corticotropin-releasing factor; oCRF, ovine CRF; h/r/mCRF, human/rat/mouse CRF; CRF receptor types 1 and 2, CRF-R1 and CRF-R2; IR, immunoreactivity; EGTA, ethylene glycol bis(2-aminoethylether)-N,N,N′,N′-tetraacetic acid; MSH, melanocyte-stimulating hormone; POMC, proopiomelanocortin; RP-HPLC, reversed-phase high performance liquid chromatography; TFA, trifluoroacetic acid; hCRF(Ox), methionine sulfoxide analog of hCRF; RIA, radioimmunoassay; RT-PCR, reverse transcriptase-polymerase chain reaction; FNB, follicular neural network B.

β-endorphin (cf. refs 3, 12). In addition, human skin can express CRF and CRF-R1 mRNA (10). To further explore this hypothesis in a model system for developmentally controlled epithelial-mesenchymal-neuroectodermal interaction, we studied CRF and CRF-R expression during the depilation-induced hair cycle in the C57BL/6 mouse (13–16).

The hair cycle is characterized by three rhythmically interchanging stages: resting (telogen), growth (anagen), and regression (catagen) (14, 17). In mice, hair follicle cycling is highly synchronized and is associated with profound changes in the architecture and physiology of all skin compartments, including skin pigmentary, endocrine, and immune systems (11, 14–21). Murine skin transcription and translation of the POMC gene, accumulation of POMC-derived neuropeptides like β-endorphin, and expression of the receptors for some POMC-derived peptides are all hair cycle dependent (11, 20, 22).

In this study, we have further explored the hypothesis that CRF and functional CRF-R proteins are expressed in mammalian skin as part of a cutaneous equivalent of a hypothalamus-pituitary axis (4). Therefore, cutaneous CRF and CRF-R expression was examined on the molecular and cellular levels during the induced hair cycle in C57BL/6 mice.

MATERIALS AND METHODS

Materials

Ovine (o) CRF, human (h) CRF, $hCRF_{16–41}$, $[Gly^{42}]$-$hCRF_{31–42}$, $[Gly^{11}]$-$hCRF_{1–11}$, $[Gly^{26}]$-$hCRF_{16–26}$, $[Gly^{31}]$-$hCRF_{21–31}$, and $[Gly^{36}]$-$hCRF_{26–36}$ were synthesized by solid-phase methodology (23, 24) and were kindly provided by Dr. M. Beyermann and Dr. J. Eichler (Institute of Molecular Pharmacology, Berlin). hCRF(Ox) (methionine sulfoxide analog of hCRF) was synthesized as described (23, 24). ^{125}I-$[Tyr^{0}]$-oCRF (81.4TBq/mmol) was obtained from DuPont NEN (Bad Homburg, Germany). ^{125}I-$[His^{32}]$-hCRF (74TBq/mmol) was purchased from Amersham Buchler GmbH (Braunschweig, Germany). Bovine serum albumin (BSA) was from Gibco BRL Life Technologies (Paisley, U.K.), Triton X-100 was from Ferak (Berlin, Germany), and sheep anti-rabbit antibody was provided by Pharmacia Biosystems GmbH (Freiburg, Germany). Bacitracin and aprotinin were from Merck (Darmstadt, Germany) and ethylene glycol bis(2-aminoethylether)-N,N,N′,N′-tetraacetic acid (EGTA) was from Sigma (St. Louis, Mo.).

Animals and skin collection

Syngeneic, female C57/BL/6 mice (6 to 9 wk old) weighing 15–20 g (Charles River, Sulzfeld, Germany, or Taconic, N.Y.) were housed in community cages under a 12 h light/darkness cycle in the Virchow Hospital Animal Facilities, Berlin, or in the Albany Medical College Animal Facilities, Albany, N.Y. Mice were fed mouse chow and water ad libitum. Active hair growth (anagen) was induced in the back skin of mice in the telogen phase by depilation, as described before (13). All key hair cycle stages (14) were studied and at least five mice were used per time point. The animals were killed by cervical dislocation under overdose anesthesia; the skin was harvested at the level of subcutis and stored at −70°C until further use.

For receptor autoradiography and immunohistology, skin was harvested in parallel to the vertebral line, and a special cryoembedding technique was used to allow longitudinal sections to be cut through the entire hair follicle (19).

Peptide extraction

Peptide extraction was performed independently, in two different laboratories, using three distinct extraction protocols.

Extraction protocol #1

The harvested skin was immediately frozen in liquid nitrogen, pulverized in a mortar, and stored at −70°C until use. To prevent skin gel formation in an acidic environment (22), acetonitrile/water was used for extraction. Every extraction step was controlled by tracer experiments. Briefly, the frozen tissue was extracted in acetonitrile/H_{2O} (1/1 (v/v), 10 ml/g tissue), and heated for 10 min at 70°C in a water bath to prevent proteolytic interference during radioimmunoassay (RIA) incubation. Aliquots of 2 ml were then centrifuged at 22,000 × *g* for 15 min at room temperature. The supernatants were collected and the procedure was repeated with a 0.5 ml solvent/probe. The combined supernatants from each aliquot were evaporated in a vacuum and treated with pentane (1 ml/sample) to remove the fat. The desiccated skin extracts were stored at −70°C until use for RIA or reversed-phase high performance liquid chromatography (RP-HPLC). The extraction method described and the RIA used for h/r/mCRF allowed the separation and determination of CRF in mouse skin in femtomolar amounts with satisfactory recovery (66%) (see below).

Extraction protocol #2

Skin was homogenized on ice in 0.5% Triton X-100 in phosphate-buffed saline, pH 7.4, containing 1 mM phenylmethylsulfonyl fluoride and 0.01% aprotinin (Sigma), as previously described (15, 21). The extracts were centrifuged at 16,000 × *g* for 30 min at 4°C. The supernatants were collected and purified through SEPCOL-1 containing 200 mg of C18, according to the manufacturer's protocol (Cat No. RIK-SEPCOL1, Penninsula, California) (25). The purified peptide-containing fractions were stored at −70°C until use.

Extraction protocol #3

Plasma (1 ml) was extracted in 1 ml acetonitrile/H_20 (1/1 (v/v), containing 0.1% trifluoroacetic acid (TFA)/0.01% Triton X-100), and heated for 10 min at 95°C in a water bath. After centrifugation at 22,000 × *g* for 15 min at room temperature, the supernatant was collected and the procedure was repeated with a 0.5 ml solvent. The combined supernatants were evaporated in a vacuum and stored at −70°C until use.

Radioimmunoassay

Immediately before RIA (26), the acid-extracted skin fractions were resuspended in 300 μl 0.066 M phosphate buffer, pH 7.4, containing 0.12 M NaCl, 0.1% NaN_3, 0.1% BSA, and 0.1% Triton X-100 (RIA buffer), sonicated for 7 min, incubated at 4°C for 1 h, and centrifuged at 22,000 × *g* for 15 min at 4°C. The pellets were resuspended in 225 μl of RIA buffer and treated as described above. Both supernatants were combined and used for RIAs. Standard hCRF in the range of 0.3—52

fmol/tube or reconstituted skin extracts were preincubated with antiserum RII (100 µl, 1:30,000) for 20 h at 4°C (final volume 500 µl). Then 100 µl of hCRF tracer (7,000–10,000 cpm) was added, followed by incubation for 48 h at 4°C. To separate the free and antibody-bound tracer fraction, 250 µl of the suspension of a solid phase-bound sheep anti-rabbit antibody was added and the mixture was incubated for 45 min at 4°C. After centrifugation (4200×*g*, 10 min, 4°C), the supernatants were aspirated. The radioactivity of the bound tracer in the sediment was counted in a Gamma Counter 1470 Wallac Wizard (Wallac Oy, Turku, Finland).

The rabbit antiserum RII used was directed toward the carboxyl-terminal sequence of hCRF and cross-reacted with hCRF(Ox), $hCRF_{16-41}$ (100%), $[Gly^{42}]$-$hCRF_{31-42}$ (0.05%), oCRF (0.06%), carp urotensin (0.005%), and frog sauvagine (1.8%). None of the following showed any cross-reactivity (less than 0.002%): partial sequences $[Gly^{11}]$-$hCRF_{1-11}$, $[Gly^{26}]$-$hCRF_{16-26}$, $[Gly^{31}]$-$hCRF_{21-31}$, $[Gly^{36}]$-$hCRF_{26-36}$, the related peptide urocortin, the peptide hormones somatostatin, thyrotropin-releasing hormone, growth hormone-releasing factor, luteinizing hormone-releasing hormone, substance P, Leu-enkephalin, Met-enkephalin, human β-endorphin, β-casomorphin, angiotensin I, human growth hormone, thyroid-stimulating hormone, follicle-stimulating hormone, luteinizing hormone, human chorionic gonadotropin, ACTH, α-MSH, and β-lipotropic hormone (24, 26). Tracer (50–60%) was bound by the antiserum RII in a final dilution of 1:180,000.

The detection limit was 0.6 fmol hCRF per tube, and the 50% intercept was at 5.6 fmol/tube. The intra-assay coefficients of variation at 2.9, 5.4, 9.0, and 18.9 fmol hCRF/tube were 5.6, 3.3, 3.5, and 3.6%, respectively, and the corresponding interassay coefficients of variation were 9.9, 8.8, 7.7, and 6.7%, respectively. Parallelism was demonstrated between the standard curve and dilution curves of CRF-IR-containing tissue extracts.

In some experiments (monitoring of the RP-HPLC separated fractions for CRF) we used a commercially available RIA kit (25) from Advanced ChemTech (Louisville, Ky.; cat# JRR2171). The assays were done according to the manufacturer's protocol. The minimum detectable sensitivity of the CRF was 2.7 fmol/tube. The cross-reactivity of the CRF antibody with CRF from human/rat was 100%; with bovine or ovine, it was 0.1%. The antibody did not cross-react with $preproCRF_{125-151}$ (human), urocortin (rat), urotensin I (catostomus commersoni), ACTH, $[Arg^8]$-vasopressin, or BNP-45 (rat). The intra- and interassay variation coefficients were below 4.9% and 12.7%, respectively.

Quantitative CRF receptor autoradiography

Cryosections of C57BL/6 back skin were prepared as described (19). As positive controls, pituitary glands from male Wistar rats were isolated and treated in the same way as the mouse skin. Sections of skin (10 µm) were cut using a cryostat microtome, thaw-mounted on aminosilan-coated slides, and stored at −80°C until use. On the day of assay, slides were brought to room temperature, preincubated for 15 min at room temperature in 50 mM Tris/HCl (pH 7.2), 10 mM $MgCl_2$, 2 mM EGTA, 0.15 mM bacitracin, 0.0015% aprotinin, and 0.1% BSA (assay buffer), and washed twice for 30 s in the same buffer. Sections were then incubated in assay buffer with 0.1 nM ^{125} I-$[Tyr^0]$-oCRF in the absence and presence of different concentrations (0.1 nM up to 1 µM) oCRF at 25°C for 2 h. Nonspecific tracer binding was determined in the presence of 1 µM oCRF. At the end of incubation, the slides were consecutively washed four times for 30 s in ice-cold assay buffer (without bacitracin, aprotinin, or BSA) containing 0.01% Triton X-100, dipped twice in deionized water, and dried rapidly under a constant stream of cold air. Slides were then apposed together with a ^{125}I-labeled standard (autoradiographic ^{125} I microscales, Amersham International, Buckinghamshire, England) to imaging plates (BAS-UR, Fuji Photo Film Co., Ltd, Tokyo, Japan) for 18 h.

Autoradiograms from the imaging plates were generated using the bioimaging analyses system BAS 3000 (Fuji Photo Film Co., Ltd, Tokyo, Japan) and quantified with the image analysis system MCID (Imaging Research Inc., St. Catharines, Ontario, Canada). The optical density of each labeled skin section was measured and converted to desintegrations per min/mg tissue equivalent, using a standard curve generated by ^{125}I-labeled standards. Receptor affinity ($K_d=1/K_{ass}$) was estimated according to the nonlinear least squares curve fitting program RADLIG (Biosoft, Cambridge, England).

After imaging plate autoradiography, the slides were dipped in Ilford Nuclear Research emulsion L4, dried at room temperature for 2 h, and stored for 2 wk with desiccant at 4°C in order to determine the localization of tracer binding at light microscopic level. Then the autoradiograms were developed (Kodak D 19 (1:1)), and the sections were stained with hematoxylin and eosin.

Reverse-phase high performance liquid chromatography

Skin extracted with acetonitrile (heating as in protocol #1) and peptide preparations obtained by purification of detergent-extracted skin throughout SEPCOL-1 (protocol #2) were each independently subjected to RP-HLPC. The extracts were separated by RP-HPLC on a Jasco gradient HPLC system (two 980 pumps; Jasco GmbH, Germany), using a PolyEncap A300 column (250×4.6 mm i.d., 5 µm; Bischoff Analysentechnik GmbH, Leonberg, Germany). The sample was dissolved in 0.1% TFA in 5% acetonitrile/95% water containing 0.01% Triton X-100, centrifuged in microfuge, and supernatants were used for injection; the injection volume was 200 µl. Mobile phase A was 0.1% TFA in water and phase B was 0.1% TFA in 80% acetonitrile/20% water (v/v). Separations were performed at a flow rate of 1 ml/min at ambient temperature, using a linear gradient 5–95% B for 40 min. Fractions of the eluent were collected with a GradiFrac (Pharmacia Biotech, Uppsala, Sweden) at 1 min intervals in polypropylen tubes and subsequently evaporated in a Speed Vac concentrator (Alpha 2–4, Christ, Osterode, Germany). After reconstitution in the buffer, fractions were monitored for CRF by the RIA assay described above.

The peptides purified by SEPCOL-1 (C18 resin, 200 mg) were dissolved in HPLC grade water containing 0.1% TFA and injected (100 µl) into a Beckman Ultrasphere C18 IP HPLC column (150×4.6 mm, 5 µm particle size) (25). An ISCO Dual Pump Model 2350 HPLC system with an ISCO V_4 variable wavelength UV detector was used to separate the peptides. The flow rate was 1 ml/min, and 1 min fractions were collected. A linear gradient of 20 to 47% acetonitrile in 0.1% TFA over a period of 45 min was used to elute neuropeptides (25). The elution time had been standardized with synthetic h/rCRF peptide. The eluted fractions were lyophilized; after reconstruction in the buffer, they were assayed with the use of a CRF RIA kit (Advanced ChemTech, Louisville, Ky.) according to the manufacturer's protocol.

Reverse transcriptase-polymerase chain reaction (RT-PCR) assays

Synthesis of the cDNA from 0.5 µg of poly $(A)^+$ mRNA or 2 µg of total isolated from skin, brain, and pituitary was performed as previously described (11). The 581 kb fragment derived from the coding region of the murine CRF exon 1–2

was amplified as previously described (11, 27). The primer sequences to amplify the cDNA fragment of 775b from the coding region of CRF-R2 were 5′ GAGACCGTGCCCCGAGTA 3′ (sense primer) and 5′ CAACAGGGGGAGGAGGAC 3′ (antisense primer). CRF-R2 cDNA was amplified 35 cycles for 1 min at 94°C, 1 min at 60°C, and 2 min at 72°C, with a final extension of 7 min at 72°C. PCR reaction contained 1× PCR buffer Perkin Elmer (2.5 mM MgCl2), 500 nM of the primers, 250 nM of dNTPs, and 1U of Amplitaq (Perkin Elmer). As a negative control, RNA samples that were not reverse transcribed were run in parallel. The reverse transcribed pituitary and brain were used as positive controls. The PCR products were separated electrophoretically on 1.5% agarose gels, stained with ethidium bromide, and photographed under UV.

To confirm specificity, the products of RT-PCR were transfered to nylon membranes (Oncor, Gaithersburg, Md.) and hybridized with the ^{32}P-labeled murine CRF cDNA (gift of Dr. J. Majzub, Children's Hospital, Boston, Mass.), as previously described (11, 27).

Immunohistochemistry

Immunohistochemical detection of CRF and CRF-R1 was carried out using rabbit antiserum against CRF (Euro-Diagnostica AB, Malmo, Sweden or Penninsula Lab, Calif.) and goat antiserum against an epitope corresponding to amino acids 425–444 mapping at the carboxyl terminus of the CRF-R1 precursor (Santa Cruz Biotechnology, Santa Cruz, Calif.), following protocols previously described (28, 29). Acetone-fixed cryostat sections were used for the analysis of CRF and CRF-R1 distribution in C57BL/6 mouse skin.

Sections fixed for 10 min at −20°C in acetone were incubated with anti-CRF and anti-CRF-R1 antibodies (dilution 1:50 and 1:100, respectively) overnight at room temperature, followed by incubation with tetramethylrhodamine-isothiocyanate-conjugated F(ab)$_2$ fragments of a goat anti-rabbit IgG (1:200 dilution, 1 h, 37°C) (Jackson ImmunoResearch Inc., West Grove, Pa.) or with biotinylated swine anti-goat IgG (1:200 dilution, 1 h, room temperature) (Cedarlane, Hornby, Canada), respectively. In the former case, the immunodistribution of CRF antigen was analyzed by fluorescence microscopy. In the latter, the CRF-R1 binding immunocomplexes were detected by using a streptavidine-alkaline phosphatase (1:500) amplification kit and examined by light microscopy.

Each immunoreactivity pattern was analyzed in at least 20 hair follicles per mouse, using at least five mice per hair cycle stage, and was recorded in a standarized, computer-generated scheme of the murine hair cycle (30). Preincubation of antiserum against CRF with 50 μg/ml of CRF peptide (Sigma St. Louis, Mo., or Penninsula, Calif.) or incubation with nonimmune serum was used as a negative control. Immunohistochemical detection of both antigens in embryonic mouse brain was used as a positive control. The micrographs were prepared using the digital image analysis system ISIS (29, 30).

RESULTS

Hair cycle-dependent CRF peptide expression in mouse skin

To identify CRF peptide in adolescent C57BL/6 back skin homogenates, we used two independent extraction protocols: an extraction with acetonitrile/water, and a detergent extraction technique with subsequent SEPCOL-1 purification. Both extracts were analyzed independently by RP-HPLC, and the collected fractions were tested using specific anti-CRF RIA. Using the former extraction protocol, we have identified the major CRF-like IR eluting at the same time as synthetic CRF standard (25 min), preceded by a minor peak eluting at 22 min that corresponded to the elution time of CRF(Ox) (**Fig. 1**).

The presence of CRF in murine skin was fully confirmed by independent RP-HPLC separations of SEPCOL-1-purified anagen III-IV and VI skin extracts and identification of CRF-IR with a commercially available CRH RIA kit (**Fig. 2**). Again, we detected a major CRF-IR eluting at the same time as CRF standard, 31 min (Fig. 2). No specific IR was detected by anti-CRF antibody in these extracts at elution times that corresponded to urocortin, urotensin, and sauvagine peptides either in combined anagen III-IV (Fig. 2) or anagen VI skin.

The concentration of CRF immunoreactive peptide was measured in mouse skin of full thickness during all key phases of the murine hair cycle (**Fig. 3**).

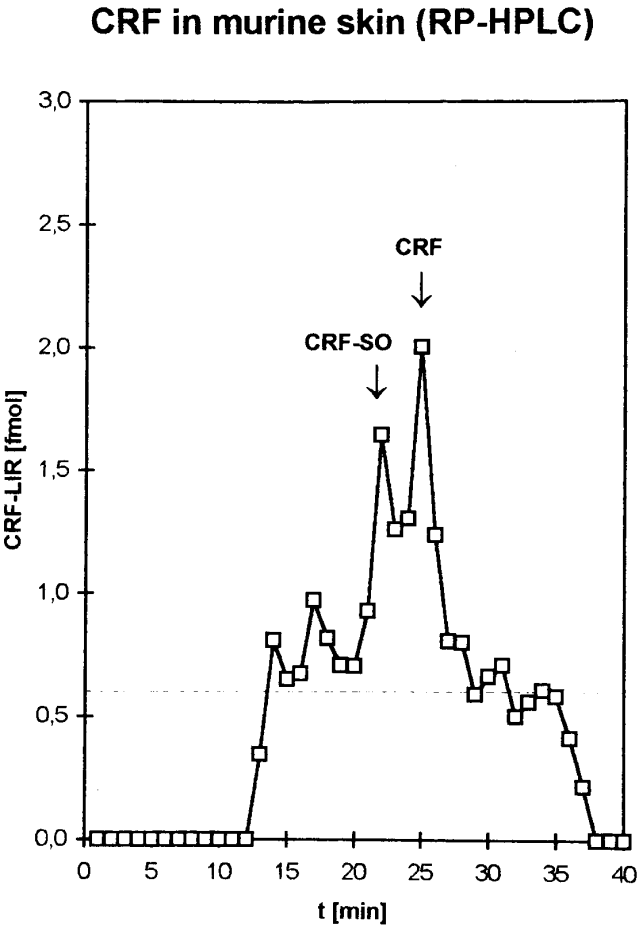

Figure 1. RP-HPLC characterization of CRF isolated from mouse skin using an acetonitrile/TFA extraction protocol (protocol #1). The CRF and CRF-S-oxide (CRF-SO) immunoreactive peaks eluted at the same time as corresponding ^{125}I-CRF (25 min) and ^{125}I-CRF-SO (22 min) tracers. RIA detection limit (- - -).

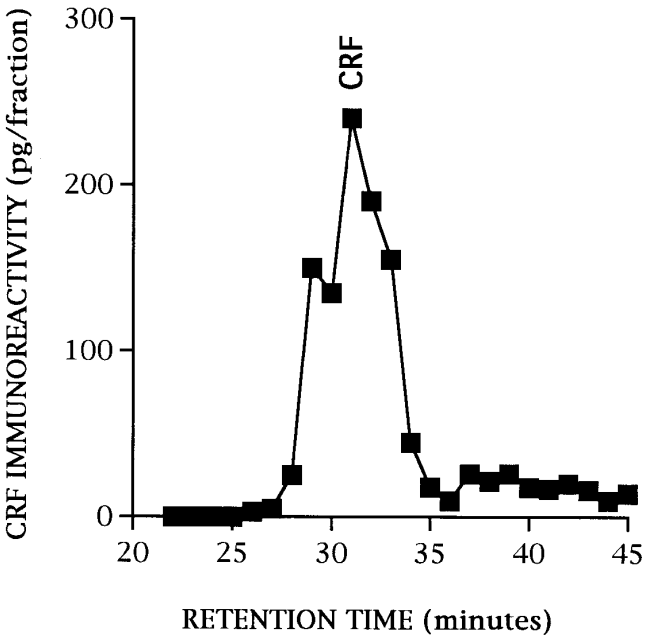

Figure 2. RP-HPLC identification of CRF immunorectivity extracted from anagen III/IV skin, using an alternative protocol (protocol #2). The radioimmunoactive peak detected by specific anti-CRF RIA kit eluted at the same time (30–31 min) as the CRF standard. Note that a different column and slightly different conditions (cf Materials and Methods) were used during this separation than in Fig. 1.

The highest CRF-IR concentrations were seen at day 5 (anagen IV) after hair depilation with 67 fmol/g wet weight tissue of skin, which significantly decreased on day 10 (anagen VI) to a level of 40 fmol/g and then reached the lowest values (36 fmol/g) in telogen skin. There were statistically significant differences between days 3 and 5, as well as between days 3 and 5 and all other days, including day 0 (telogen), when using the Student-Newman-Keuls-test ($P<0.05$).

In addition, CRF concentration in plasma was determined in telogen and anagen IV skin; their values were 5.6 and 8.6 fmol/ml plasma, respectively. For comparison, CRF concentrations reported in rat plasma were determined to be 2.0–2.8 fmol/ml (31, 32). The CRF-IR was detected at the same elution time as CRF standard by RP-HPLC (not shown). Because cutaneous CRF levels (Fig. 3) are substantially higher than CRF plasma levels, the hair cycle-dependent changes in CRF skin levels are unlikely to reflect CRF plasma changes.

Using RT-PCR, we had previously failed to detect the CRF mRNA spanning exon 1–2 region in telogen, anagen, and catagen C57BL/6 mouse skin (11). Despite an increased number of PCR cycles (up to 45) with subsequent Southern blotting, we again failed to detect a specific fragment that would hybridize with CRF cDNA prepared from mouse skin, despite its presence in the positive control mouse brain (not shown).

Identification and characterization of CRF receptors in mouse skin

Specific CRF binding sites (autoradiographic grains) were detected by autoradiography in murine skin labeled with ^{125}I-Tyr°-oCRF (**Fig. 4**). Specific and identifiable binding sites were present in the panniculus carnosus (i.e., the subcutaneous muscle layer of rodent skin), hair follicle, and epidermis. The highest concentration of CRF binding sites was detected in the panniculus carnosus (Fig. 4).

The CRF binding sites in mouse skin were determined with quantitative autoradiography by a competitive displacement assay in skin sections obtained from mice in the telogen stage. The competitive displacement of the binding of ^{125}I-[Tyr°]-oCRF in the presence of increasing concentrations of unlabeled oCRF demonstrated specific binding sites in mouse skin (**Fig. 5**). Analysis of the displacement curve revealed a single high-affinity binding site with a dissociation constant (K_d) of 3.62 nM. B_{max} determined directly from the difference of the total binding and the nonspecific binding (defined as the binding of the tracer in the presence of 1 μM oCRF) was 2.42 amol/mm^2 scanned skin section. For comparison, the binding parameters of oCRF in the rat pituitary were determined by displacement of ^{125}I-[Tyr°]-oCRF by oCRF in frozen sections, revealing that the K_d and B_{max} were 1.53 nM and 18.1 amol/mm^2, respectively (Fig. 5). Preliminary experiments showed no substantial dependence of the specific binding of ^{125}I-[Tyr°]-oCRF on the hair cycle of skin sections determined at days 0, 3, and 12 (not shown).

In situ localization of CRF and CRF-R1 antigens

Immunofluorescence studies showed hair cycle-dependent changes in the distribution of CRF-IR and CRF-R1 protein in mouse skin (**Fig. 6** and **Fig. 7**). Large nerve bundles in the dermis and subcutis displayed CRF-IR throughout the hair cycle (Fig. 6*A*). In telogen and anagen II skin, CRF-IR was localized mainly in basal layer epidermal keratinocytes and in keratinocytes of the suprainfundibular outer root sheath, as well as in keratinocytes of the bulge and the developing anagen hair bulb (Fig. 6*A* and Fig. 7). In anagen IV, CRF-IR was present in most keratinocytes of the epidermis and of the proximal outer root sheath (Fig. 6*C* and Fig. 7). CRF-IR also appeared in longitudinal and circular nerve fibers around the hair follicle isthmus (Fig. 6*C* and Fig. 7), i.e., in the so-called follicular neural network B (FNB) (29). Anagen VI hair follicles displayed CRF-IR in the proximal outer/inner root sheath and hair matrix as well as in nerve fibers of the FNB (Fig. 6*E* and Fig. 7). In catagen, CRF-IR was present in the secondary hair germ, proximal outer root sheath, and nerves around the isthmus, and disappeared in the epider-

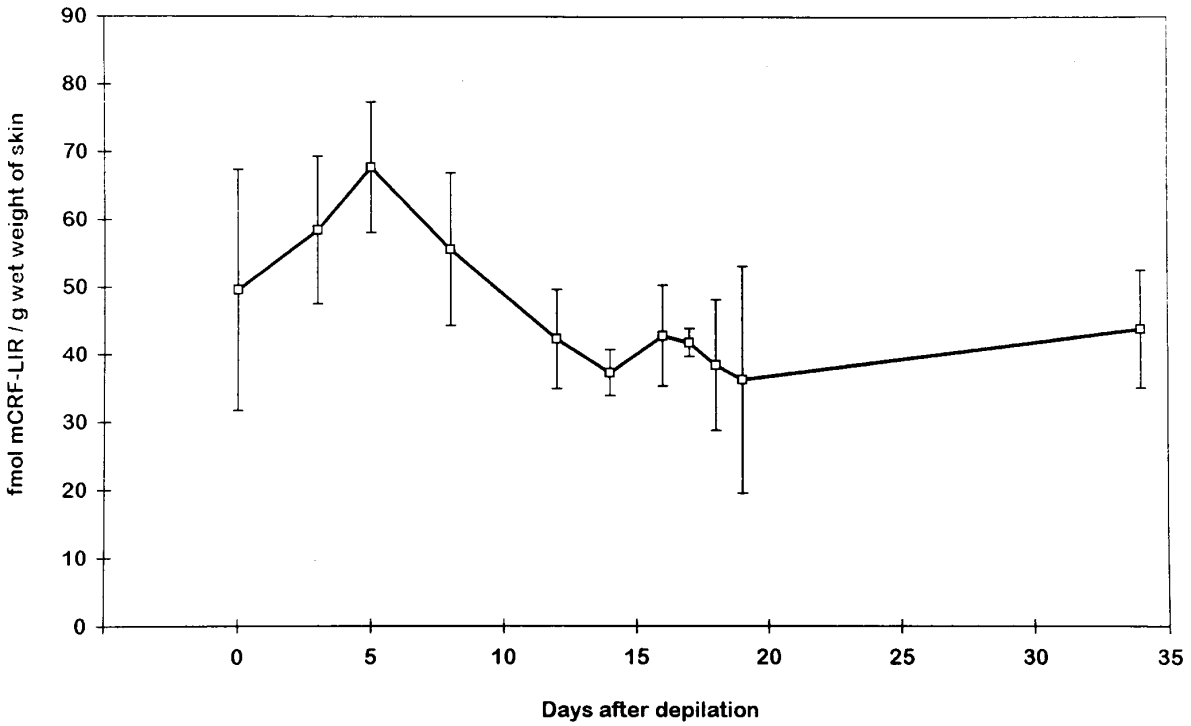

Figure 3. Changes in murine skin CRF concentration associated with synchronized hair follicle cycling. By Student-Newman-Keuls test, there are statistically significant differences between day 3 (early anagen) and day 5 (mid-anagen) and between days 3 and 5 and all other days, including day 0 (telogen); $P < 0.05$.

mis, inner root sheath, and distal outer root sheath (Fig. 6*G* and Fig. 7).

CRF-R1-IR was at the level of background in telogen skin (Fig. 6*B* and Fig. 7), whereas identifiable CRH-R1-IR began to appear in germ plate keratinocytes of the developing hair bulb of anagen II follicles. Numerous keratinocytes of the proximal inner root sheath and some keratinocytes of the proximal outer root sheath also displayed CRF-R1-IR during anagen IV (Fig. 6*D* and Fig. 7). In anagen VI, CRF-R1-IR appeared in dermal papilla fibroblasts, was present in the proximal outer and inner root sheath, but disappeared from the hair matrix (Fig. 6*F* and Fig. 7). In catagen, CRF-R1-IR was present only in keratinocytes of the regressing inner root sheath (Fig. 6*H* and Fig. 7).

DISCUSSION

We demonstrate the presence of both CRF and CRF-R antigens in C57BL/6 mouse skin. RP-HPLC and RIA analyses of skin extracts from different hair cycle stages documented the presence of CRF peptide in the skin. The amount of CRF changed with synchronized hair follicle cycling, peaking in anagen IV skin. This correlated well with the maximal CRF expression identified by immunofluorescence in anagen skin. Maximal CRF-IR was localized to the basal epidermis, the outer root sheath, and matrix region of anagen IV-VI follicles and their neural network B, whereas minimal CRF-IR was detected in catagen and telogen skin.

A question remains as to what the source of intracutaneous CRF may be. The discrepancy between the presence of peptide and an apparent absence of CRF gene expression in murine skin suggests that the identified CRF-IR may originate from an extracutaneous site of synthesis. It may be delivered to skin via descending nerve endings, as proposed previously (11). This possibility appears to be supported by the presence of CRF-IR in nerve bundles of dermis/subcutis and by positive CRF staining of longitudinal and circular FNB nerve fibers (see Fig. 6 and Fig. 7). Some CRF may also derive from the serum, but this is an unlikely possibility because plasma levels of CRF are substantially lower than the concentration of CRF in skin. The observed strong intraepithelial CRF-IR stain may then represent predominantly receptor-mediated internalization of CRF released by nerve endings. Because human skin expresses CRF, CRF-R1 mRNA (10), and CRF peptide (25), it is also possible that part of the detected CRF-IR is the product of an as yet unidentified cutaneous gene whose product shows high homology to hypothalamic CRF.

Since CRF is the major regulator of pituitary POMC gene expression and production of POMC peptides (1, 2), it is conceivable that the increased content of CRF in anagen IV is functionally linked to synthesis of the POMC protein, with subsequent pro-

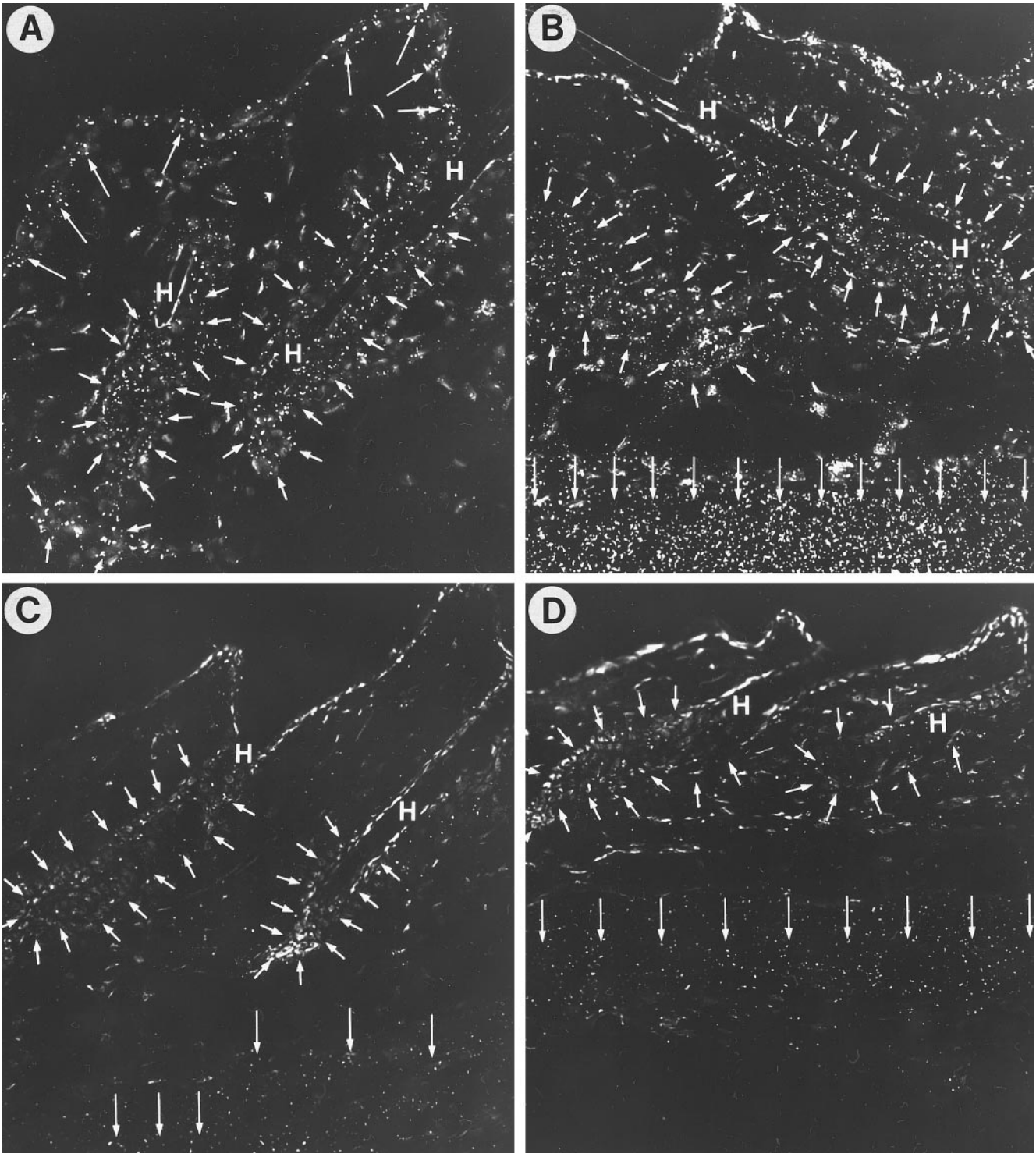

Figure 4. Autoradiographic distribution of CRF binding sites in mouse skin labeled with ^{125}I-[Tyr^0]-oCRF. *A, B*) Total binding in the presence of 0.1 nM ^{125}I-[Tyr^0]-oCRF. *C, D*) Nonspecific binding (0.1 nM ^{125}I-[Tyr^0]-oCRF in the presence of 1 μM unlabeled oCRF. Silver grains resulting from radioactivity of ^{125}I-CRF are localized in the hair follicle (short arrows), panniculus carnosus (long arrows), and epidermis (long arrows).

duction of POMC peptides such as ACTH, MSH, and β-endorphin. There is indeed hair cycle-dependent expression of POMC mRNA, protein, and POMC-derived β-endorphin in the skin of C57BL/6 mice (11, 20, 22).

Specifically, a 30 to 33 kDa POMC protein was detected in anagen IV, but not in telogen or anagen I-III skin; full-length POMC mRNA of 1.1 kb was detected only in anagen IV; truncated POMC transcripts of 0.9 kb were detected in other phases of the

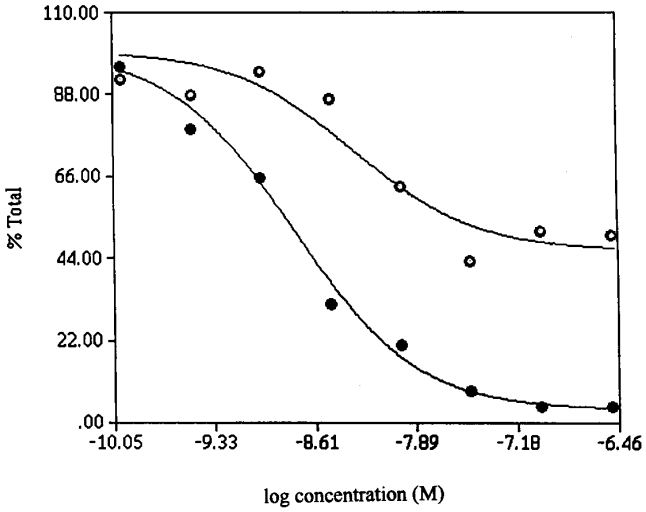

Figure 5. Competitive displacement by oCRF of ^{125}I-[Tyr^0]-oCRF bound to sections of mouse skin (○) and sections of rat pituCRF-R type 1 CRF-R type 1 itary (●). The displacement curves resulted from multifile analysis (RADLIG) of two independent binding experiments, each using six skin sections/concentration, and of three independent experiments, each using two sections of rat pituitary/concentration.

hair cycle (11, 20, 27). The progression through the hair cycle was accompanied by an increased concentration of POMC-derived β-endorphin, reaching a peak in anagen VI (22). Further support for the hypothesis that intracutaneous CRF expression may, at least in part, control local POMC (12) comes from an in situ hybridization study showing that POMC mRNA is expressed in epidermal and outer root sheath keratinocytes during anagen (33)—in those cells that displayed strong CRF-IR during anagen development.

By quantitative autoradiography, we have presented the first evidence that mammalian skin expresses high-affinity binding sites for CRF, with the highest density of specific binding sites in the panniculus carnosus, epidermis, and follicle epithelium. The high-affinity binding sites for CRF had a K_d of 3.62 nM, which is comparable to that of rat pituitary (1.53 nM) and brain (4.31 nM) (34). However, the concentration of binding sites in skin (B_{max} of 2.42 amol/mm^2) was much lower than that in the pituitary (18.1 amol/mm^2). Although this study is in general agreement with previous detection of the CRF-R1 mRNA in mouse skin (11) and the in situ localization of the CRF-R1 antigen to the hair follicle presented here, some peculiarities need to be considered.

Previously, we had detected hair cycle-dependent steady-state levels of CRF-R1 mRNA, with a maximum in anagen VI and a minimum in telogen (11). Here we show by immunohistology that the distribution of CRF-R1 antigens also changes in a hair cycle-dependent manner, since CRF-R1 immunoreactivity was absent in telogen skin and reached its highest value in anagen VI (Fig. 6 and Fig. 7). In contrast, autoradiography did not reveal striking differences in total CRF binding between telogen and anagen skin. In addition, CRF-R1 immunoreactivity in situ was located predominantly in the epithelial structures of anagen and catagen hair follicles and in the dermal papilla of anagen VI follicles, but not in the epidermis or panniculus carnosus.

This raises the question of whether, in addition to CRF-R1, other CRF receptors are expressed in murine skin. The CRF-R gene family includes at least two genes that share high sequence homology and belong to the seven-transmembrane receptor protein family coupled to the Gs signaling protein (6–9). CRF-R1 is expressed preferentially in the brain and pituitary gland, and CRF-R2β is expressed in heart and skeletal muscle (6–9). In preliminary studies, we have amplified (by using RT-PCR) an expected 775 bp fragment from the coding region of the CRF-R2 gene in mouse skin and brain. Thus, it is conceivable that mouse skin expresses more than one CRF-R gene and that the CRF-R2 gene might be expressed predominantly in the panniculus carnosus and epidermis, whereas CRF-R1 expression may predominate in the hair follicle.

The hair follicle and its cyclic growth and regression activity offer an ideal model system for studying developmentally controlled epithelial-mesenchymal-neuroectodermal interaction systems (cf. refs 14, 16, 35). Therefore, the current observations on hair cycle-dependent expression of CRF and CRF receptors in murine skin in an exceptionally well-defined and easily manipulated mouse model raise intriguing developmental questions as to the role of CRF/CRF-R-dependent signaling in the control of epithelialmesenchymal-neuroectodermal interactions in general, and in the control of epithelial tissue remodeling during morphogenesis and postnatal tissue homeostasis in particular (cf. refs 36, 37). It will now be critical to explore, for example, whether CRF-R agonists and antagonists interfere with hair follicle cycling in a manner that might be exploited therapeutically (cf. refs 14, 16), or that may provide further proof for the hypothesis that the tissue remodeling of peripheral organs can indeed be affected by interaction with the receptors for 'hypothalamic' hormones (4, 12). In addition, CRF-overproducing transgenic mice (38) and CRF-deficient knockout mice (39) that have recently become available offer instructive complementary tools for dissecting in detail how over- or understimulation of CRF receptors can affect hair follicle morphogenesis, growth, and cycling.

In conclusion, we suggest that the CRF-CRF receptor signaling system is operating in mouse skin as an additional 'neuroendocrine' pathway that regulates

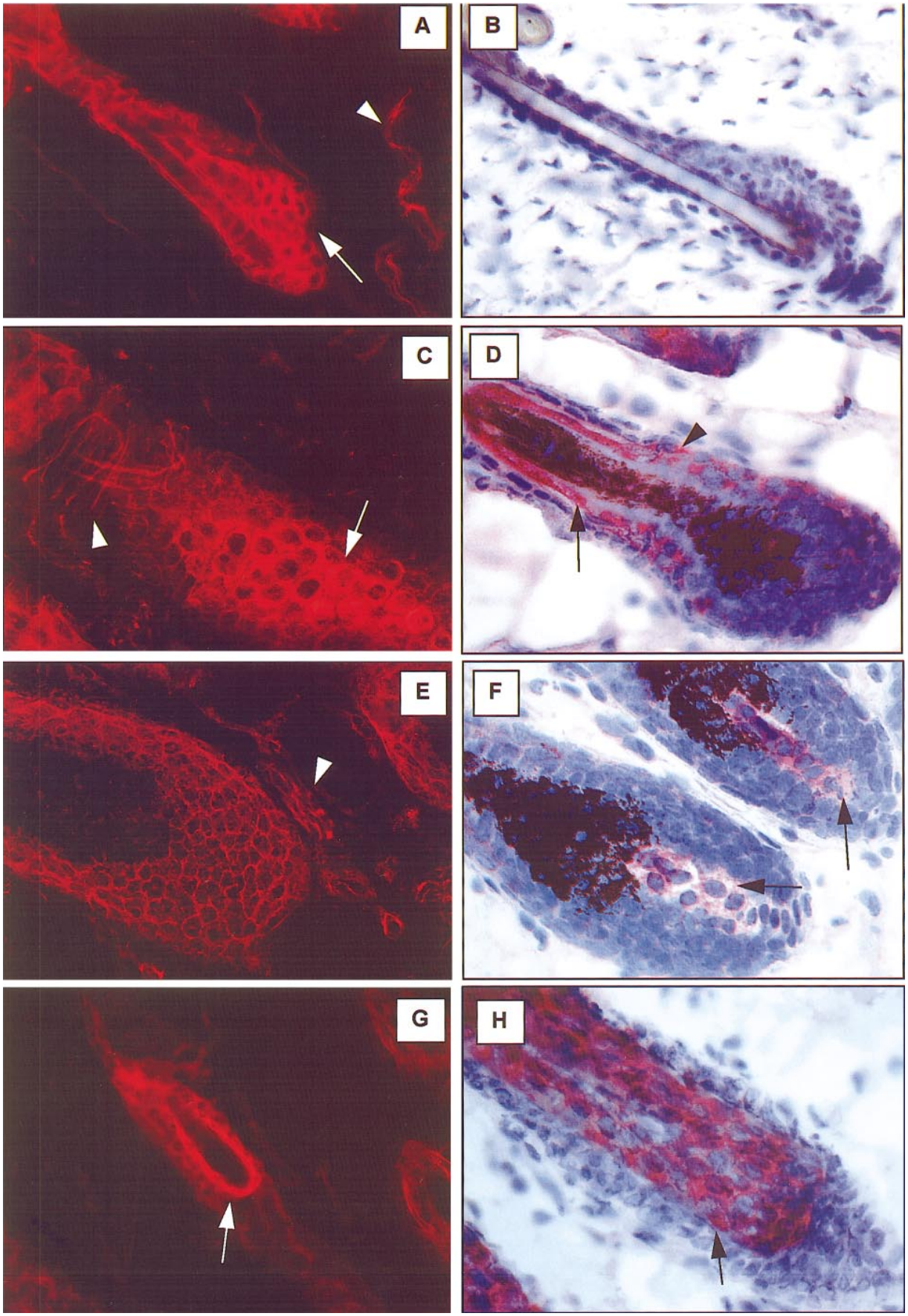

Figure 6. Immunolocalization of CRF and CRF-R1 antigens in back skin during the murine hair cycle. Cryostat sections were immunostained with antisera against CRF (indirect immunofluorecence; left column) or against CRF-R1 (immunocytochemistry; right column). Telogen (*A*, *B*); anagen IV (*C*, *D*); anagen VI (*E*, *F*); catagen (*G*, *H*). White arrowheads: CRF positive nerve bundles (*A*, *E*) and perifollicular nerve fibers (*C*). White arrows: CRF positive hair bulb keratinocytes (*A*, *C*, *E*). Black arrows: CRF-R1 positive hair bulb keratinocytes (*D*, *G*, *H*) and dermal papilla fibroblasts (*F*). ×400.

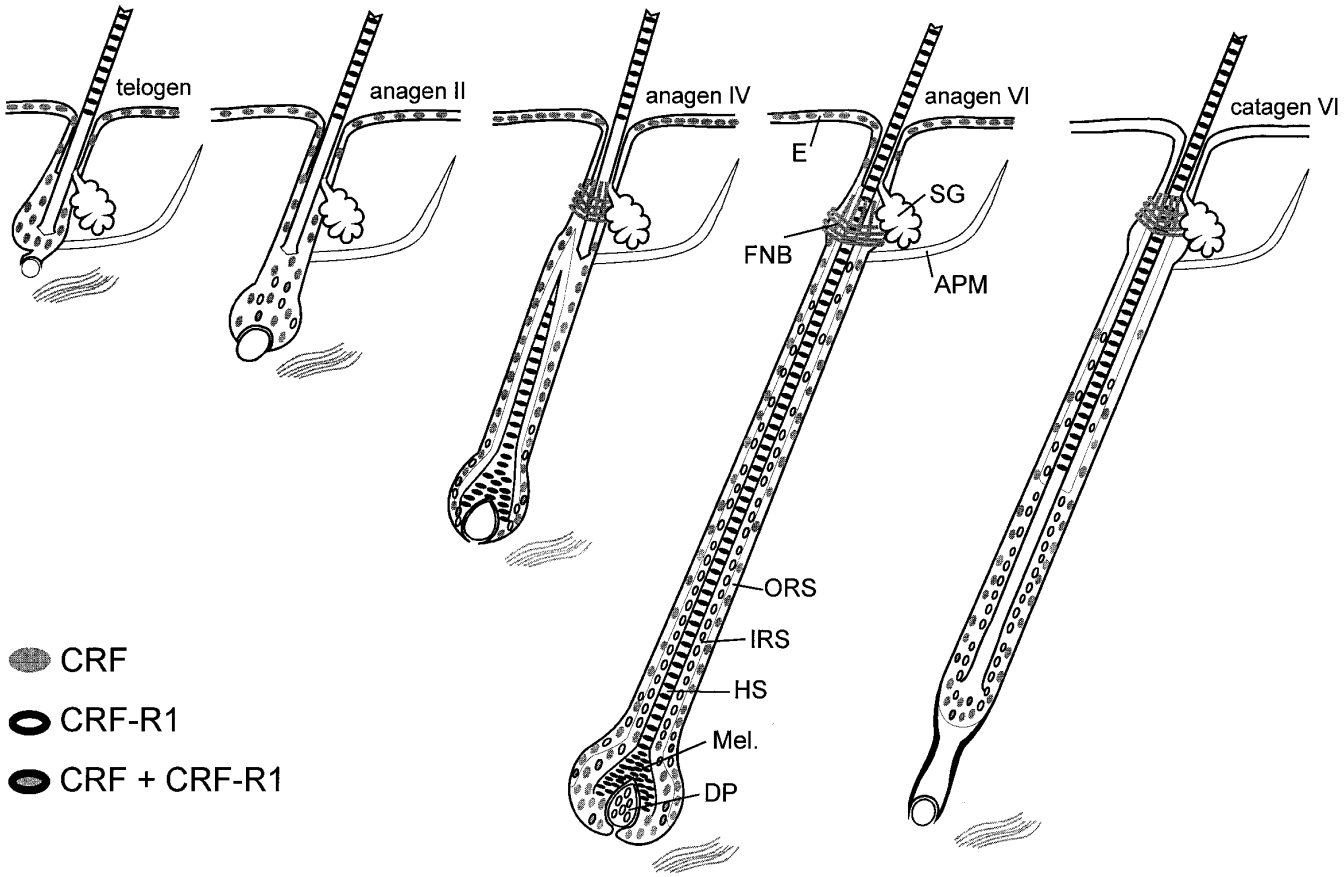

Figure 7. Schematic representation of CRF and CRF-R1 antigen expression in different skin and hair follicle compartments of adolescent C57BL/6 mouse back skin, with all hair follicles in the resting stage of the hair cycle (telogen), selected growth stages (anagen II, IV, and VI), and one selected regression stage (catagen VI). Abbreviations: APM, arrector pili muscle; DP, dermal papilla; E, epidermis; FNB, follicular network B; HS, hair shaft; IRS and ORS, inner and outer root sheath, respectively; Mel, melanocytes; SG, sebaceous gland.

skin functions, possibly in connection with cutaneous responses to various stressors (cf 4). FJ

We thank Dr. E. Fuchs (Deutsches Primaten Zentrum, GmbH, Gottingen) for his contribution in establishing quantitative CRF receptor autoradiography and J. Eichorst and G. Vogelreiter for technical assistance. The support and advice of Drs. W. Sterry, M. Bienert, and W. Rosenthal are gratefully appreciated. The work was supported in part by grants Pa 345/6–1 from Deutsche Forschungsgemeinschaft (R.P.), IBN-9604364 from the National Science Foundation (A.S.), and NMBF 011ZZ9508 and Wella AG, Dermstadt (RP).

REFERENCES

1. Hadley, M. (1996) *Endocrinology*, Prentice Hall, Englewood Cliffs, N.J
2. Orth, D. N. (1992) Corticotropin-releasing hormone in humans. *Endocrine Rev.* **13**, 164–191
3. Luger, T. A., Scholzen, T., Brzoska, T., Becher, E., Slominski, A., and Paus, R. (1997) Cutaneous immunomodulation and coordination of skin stress responses by alpha-melanocyte-stimulating hormone. *Ann. N.Y. Acad. Sci.* In press
4. Slominski, A., and Mihm, M. (1996) On a potential mechanism of skin response to stress. *Int. J. Dermatol.* **35**, 849–851
5. Shibahara, S., Morimoto, Y., Furutani, Y., Notake, M., Takahashi, K., Shimuzu, S., Horikawa, S., and Numan, S. (1983) Isolation and sequence analysis of the human corticotropin-releasing factor precursor gene. *EMBO J.* **2**, 775–779
6. Chen, R., Lewis, K. A., Perrin, M. H., and Vale, W. W. (1993) Expression cloning of human corticotropin-releasing factor receptor. *Proc. Natl. Acad. Sci. USA* **90**, 8967–8971
7. Kishimoto, T., Pearse, R. V., Lin, C. R., Rosenfeld, M. G. (1995) A sauvagine/corticotropin-releasing factor receptor expressed in heart and skeletal muscle. *Proc. Natl. Acad. Sci. USA* **92**, 1108–1112
8. Liaw, C. W., Lovenberg, T. W., Barry, G., Oltersdorf. T., Grogoriadis, E. E., and DeSouza, E. B. (1996) Cloning and characterization of he human corticotropin-releasing factor-2 receptor complementary deoxyrubonucleic acid. *Endocrinology* **137**, 72–77
9. Vita, N., Laurent, P., Lefort, S., Chalon, P., Lelias, J.-M., Kaghad, M., Le Fur, G., Caput, D., and Ferrara, P. (1993) Primary structure and functional expression of mouse pituitary and human corticotropin releasing factors receptors. *FEBS Lett.* **335**, 1–5
10. Slominski, A., Ermak, G., Hwang, J., Chakraborty, A., Mazurkiewicz, J., and Mihm, M. (1995) Proopiomelanocortin, corticotropin releasing hormone and corticotropin releasing hormone receptor genes are expressed in human skin. *FEBS Lett.* **374**, 113–116
11. Slominski, A., Ermak, G., Hwang, J., Mazurkiewicz, J., Corliss, D., and Eastman, A. (1996) The expression of proopiomelanocortin (POMC) and of corticotropin releasing hormone receptor (CRH-R) genes in mouse skin. *Biochim. Biophys. Acta* **1289**, 247–251
12. Slominski, A., Paus, R., and Wortsman, J. (1993) On the potential role of proopiomelanocortin in skin physiology and pathology. *Mol. Cell. Endocrinol.* **93**, C1–C6
13. Paus, R., Stenn, K., and Link, R. E. (1990) Telogen skin contains an inhibitor of hair growth. *Br. J. Dermatol.* **122**, 777–784

14. Paus, R. (1996) Control of the hair cycle and hair diseases as cycling disorders. *Curr. Opin. Dermatol.* **3**, 248–258
15. Slominski, A., Paus, R., and Costantino, R. (1991) Differential expression and activity of melanogenesis-related proteins during induced hair growth in mice. *J. Invest. Dermatol.* **96**, 172–179
16. Slominski, A., and Paus, R. (1993) Melanogenesis is coupled to murine anagen: Toward new concepts for the role of melanocytes and the regulation of melanogenesis in hair growth. *J. Invest. Dermatol.* **101**, 90S–97S
17. Chase, H. B. (1954) Growth of the hair. *Physiol. Rev.* **34**, 113–126
18. Hoffmann, U., Tokura, Y., Nishijima, T., Takigawa, T., and Paus, R. (1996) Hair cycle-dependent changes in skin immune functions: anagen associated depression of sensitization for contact hypersensitivity in mice. *J. Invest. Dermatol.* **106**, 598–604
19. Paus, R., Hofmann, U., Eichmueller, S., and Czarnetzki, B. M. (1994) Distribution and changing density of gamma-delta T cells in murine skin during the induced hair cycle. *Br. J. Dermatol.* **130**, 281–289
20. Slominski, A., Paus, R., and Mazurkiewicz, J. (1992) Proopiomelanocortin expression in the skin during induced hair growth in mice. *Experientia* **48**, 50–54
21. Slominski, A., Paus, R., Plonka, P., Maurer, M., Chakraborty, A., Pruski, D., and Lukiewicz, S. (1994) Melanogenesis during the anagen-catagen-telogen transformation of the murine hair cycle. *J. Invest. Dermatol.* **102**, 862–869
22. Furkert, J., Klug, U., Slominski, A., Eichmueller, S., Mehlis, B., Kertscher, U., and Paus, R. (1997) Identification and measurement of β-endorphin levels in the skin during induced hair growth in mice. *Biochim. Biophys. Acta* **1336**, 315–322
23. Beyermann, M., Fechner, K., Furkert, J., Krause, E., and Bienert, M. (1996) A single point sligth alteration set as a tool for structure-activity relationship studies of ovine corticotropin releasing factor. *J. Med. Chem.* **39**, 3324–3330
24. Eichler, J., Furkert, J., Bienert, M., Rohde, W., and Lebl, M. (1991) Multiple peptide synthesis on cotton carriers—elucidation and characterization of an antibody binding site of CRF. In *Peptides 1990* (Giralt, E., and Andreu, D., eds) pp. 156–157, ESCOM, Leiden
25. Slominski, A., Baker, J., Ermak, G., Chakraborty, A., and Pawelek, J. (1996) UVB stimulates production of corticotropin releasing factor (CRF) by human melanocytes. *FEBS Lett.* **399**, 175–176
26. Rückert, Y., Rohde, W., and Furkert, J. (1991) Radioimmunoassay of corticotropin-releasing hormone. *Exp. Clin. Endocrinol.* **96**, 129–137
27. Ermak, G., and Slominski, A. (1997) Production of POMC, CRH-, ACTH- and α-MSH-receptor mRNA and expression of tyrosinase gene in relation to hair cycle and dexamethasone treatment in the C57BL/6 mouse skin. *J. Invest. Dermatol.* **108**, 160–167
28. Eichmueller, S., Stevenson, P. A., and Paus, R. (1996) A new method for double immunolabeling with primary antibodies from identical species. *J. Immunol. Methods* **190**, 255–265
29. Botchkarev, V. A., Eichmueller, S., Johansson, O., and Paus, R. (1997) Hair cycle-dependent plasticity of skin and hair follicle innervation in normal murine skin. *J. Comp. Neurol.* **386**, 379–385
30. Paus, R., Foitzik, K., Welker, P., Bulfone-Paus, S., and Eichmueller, S. (1997) Transforming growth factor-beta type I and type II receptor expression during murine hair follicle development and cycling. *J. Invest. Dermatol.* **109**, 518–526
31. Nishioka, T., Iyota, K., Takao, T., Suemaru, S., Numata, Y., and Hashimoto, K. (1994) Plasma CRH response to water immersion-restraint stress in rats bearing a hypothalamic knife cut. *Endocrinol. J.* **41**, 453–459
32. Plotsky, P. M., Otto, S., Toyama, T., and Sutton, S. (1990) Lack of correlation between immunoreactive corticotropin-releasing factor concentration profiles in hypophysial-portal and peripheral plasma. *J. Neuroendocrinol.* **2**, 65–69
33. Mazurkiewicz, J. E., Corliss, D., Ermak, G., and Slominski, A. (1996) Differential expression of POMC mRNA and POMC peptides during the hair cycle in mouse. *J. Histochem. Cytochem.* **44**, 784A (abstr.)
34. Rohde, E., Furkert, J., Fechner, K., Beyermann, M., Mulvany, M. J., Richter, R. M., Denef, C., Bienert, M., and Berger, H. (1996) Corticotropin-releasing hormone (CRH) receptors in the mesenteric small arteries of rats resemble the (2)-subtype. *Biochem. Pharmacol.* **52**, 829–833
35. Paus, R., Peters, E. M. J., Eichmueller, S., and Botchkarev, V. A. (1997) Neural mechanism of hair growth control. *J. Invest. Dermatol. Sympos. Proc.* **2**, 61–68
36. Gilbert, S. F. (1994) *Developmental Biology of the Skin*, Sinauer, Sunderland, Massachusetts
37. Mueller, W. A. (1997) *Developmental Biology*, Springer, New York, New York
38. Stenzel-Poore, M. P., Duncan, J. E., Rittenberg, M. B., Bakke, A. C., and Heinrichs, S. C. (1996) CRH overproduction in transgenic mice: behavioral and immune system modulation. *Ann. N.Y. Acad. Sci.* **780**, 36–48
39. Muglia, L., Jacobson, L., and Majzoub, J. A. (1996) Production of CRH-deficient mice by targeted mutation in embryonic stem cells. *Ann. N.Y. Acad. Sci.* **780**, 49–59

Received for publication September 12, 1997.
Accepted for publication November 10, 1997.